

NLO predictions for a lepton, missing transverse momentum and dijets at the Tevatron

John M. Campbell, Adam Martin and Ciaran Williams

Fermilab National Accelerator Laboratory

Batavia, Illinois

USA 60510.

(Dated: April 17, 2018)

In this letter we investigate the various processes that can contribute to a final state consisting of a lepton, missing transverse momentum and two jets at Next to Leading Order (NLO) at the Tevatron. In particular we consider the production of $W/Z + 2$ jets, diboson pairs, single top and the $t\bar{t}$ process with both fully leptonic and semi-leptonic decays. We present distributions for the invariant mass of the dijet system and normalisations of the various processes, accurate to NLO.

PACS numbers:

INTRODUCTION

CDF has recently reported an excess in the dijet invariant mass distribution around 150 GeV for events containing a lepton, missing energy and exactly two jets [1]. This has led to many new physics interpretations [2–20] as well as some suggestions that the excess can be explained within the framework of the Standard Model (SM) [21, 22]. Both of the proposed Standard Model explanations require changes in the normalisation of backgrounds containing top quarks, which could be the result of higher order perturbative corrections that have not been fully accounted for in the analysis. In this letter we investigate this issue by performing a NLO study of SM processes that can produce the final state of interest. We investigate the cross sections and invariant mass distributions under the CDF cuts and assign an estimate of the corresponding theoretical uncertainty. To provide a further calibration of these processes, we vary the cuts by allowing additional jets in the final state and by changing the minimum jet transverse momentum (p_T).

DESCRIPTION OF THE CALCULATION

We present results for NLO cross sections using the latest version (v6.0) of MCFM [23]. This includes NLO contributions to the production of $V + 2$ jets (where $V = W, Z$), VV [29], $t\bar{t}$ and single top. The current implementation of MCFM does not include radiation of gluons from quarks produced in the decay of vector bosons or top quarks. Such contributions should not lead to additional peaks in the dijet invariant mass distribution, particularly in the region of interest, and we expect that our current implementation provides a satisfactory description of any potential features in these processes.

We perform our calculation using the cuts described in ref. [1]. Namely, we ask for events containing exactly two jets with $p_T^j > 30$ GeV in $|\eta^j| < 2.4$ units of rapidity. We use the k_T algorithm with parameter $R = 0.4$, but have checked that differences with the cone algorithm are small. The jets must be separated by at most 2.5 units of rapidity and the

transverse momentum of the dijet system (p_T^{jj}) is constrained by $p_T^{jj} > 40$ GeV. Events should contain exactly one lepton in $|\eta^\ell| < 1$, $p_T^\ell > 20$ GeV that is separated from the jets by $R_{j\ell} > 0.52$. We require that the missing transverse momentum (E_T^{miss}) satisfies $E_T^{\text{miss}} > 25$ GeV and is separated azimuthally from the leading jet, $\Delta\phi > 0.4$.

We evaluate cross sections using the MSTW08 PDF set [24] (matched to the appropriate order in perturbation theory), using the default set of electroweak parameters in MCFM [23]. For simplicity we choose to evaluate all of the processes at a scale of $2m_W$. Such a scale is motivated by its proximity to both the top mass and the region of the observed excess. In the estimate of the theoretical uncertainty we vary this by a factor of two in each direction, thus encompassing many typical scale choices for each of the processes considered.

For the vector boson decays we include two families of leptons (e and μ) in each process. When there are two leptons present (such as in $Z + 2$ jets) we require that one lepton satisfies the rapidity and momentum cuts and the other is missed to provide a source of E_T^{miss} . Jets that do not lie within our acceptance are not included as missing energy. For the $W(\ell\nu)Z(q\bar{q})$ process we impose an artificial $m_{q\bar{q}} > 10$ GeV cut in order to avoid the production of real photons, a contribution that should be included in the QCD background that we do not attempt to model here. We have checked predictions for the dijet invariant mass from single top production using both the four and five flavour schemes at LO and observe no distinctive shape difference between the two. The results presented in this paper are in the five-flavour scheme, which yields a larger cross section and could therefore be viewed as the more conservative choice.

RESULTS

In Table I we present the results for cross sections obtained using the CDF cuts described in the previous section. We show results for each contribution separately at LO and NLO and also the ratio of NLO to LO (the K -factor). We find that under the cuts the NLO corrections to many of the processes are relatively small, i.e. the K -factors are close to unity. The

exceptions to this are the diboson processes, which all receive corrections larger than 50% due to the introduction of events where one of the hard jets arises from the real radiation. At NLO the estimated theoretical uncertainty is 11% or less for all processes. The invariant mass of the dijet system is depicted in Fig. 1, where we observe that above the W and Z resonance region the $W + 2$ jets process is a falling distribution while the top contribution peaks around 140 GeV. The $Z + 2$ jets process has the same shape as the $W + 2$ jets background.

Applying the two-jet exclusivity requirement in our fixed order calculation leaves the predictions susceptible to potentially-large logarithms and significant higher-order corrections. For this reason, in Table II we also present results for cross sections at NLO using the same cuts as before, but without the two-jet exclusivity requirement (“inclusive”). For these results the jet cuts described earlier apply only to the two hardest jets. At LO this only affects $t\bar{t}$ production with semi-leptonic decays since this process contains four partons. Dropping the 2-jet requirement increases the cross section by around a factor of seven. For all processes, additional radiation present in the NLO calculations is no longer cut away, resulting in larger K -factors. The estimated uncertainty from scale variation is very similar to the exclusive case. The invariant mass of the two hardest jets is presented in Fig. 2, where the increase in the top background is clear. Moreover, there is a clear kinematic feature in the top backgrounds in the region of 150 GeV. This edge arises from the semi-leptonic decay of a $t\bar{t}$ pair, as pointed out in ref. [21] in the context of a source for the CDF excess. In the total m_{jj} distribution this edge manifests itself as a change in shape either side of 150 GeV. We note that the shape of the $W +$ jets background is relatively stable when going from the exclusive to inclusive cuts.

To further study the relative importance of the top background we present results for the cross sections and m_{jj} distribution with an increased minimum jet- p_T cut in Table III and Fig. 3. Here we use the same inclusive cuts but increase the minimum jet p_T to 40 GeV. This results in a further enhancement of the top background and a clear peak in the total SM distribution in the 100 – 150 GeV region. The shape of the $W +$ jets background has altered significantly as a result of the increased cuts, also peaking around 140 GeV. Therefore, although these cuts may be useful to constrain the normalisation of the SM backgrounds, they may lead to a reduction in significance of any potential signal in this region.

In ref. [21] the SM peak in the top distribution was suggested as an explanation of the CDF excess. We note that the peak in the top contribution at m_W is correlated with the feature at 140 GeV since they both arise solely from semi leptonic $t\bar{t}$ events. Since, under the inclusive cuts, a large fraction of the total W peak is comprised of top events, one would expect good control of the top normalisation if the W peak is well-described. One way that the top background normalisation could be constrained would be to observe and measure the W resonance with inclusive cuts, particular with a higher

Process	σ^{LO} [fb]	σ^{NLO} [fb]	Ratio (NLO/LO)
$W + 2j$	4984(8) $^{+41\%}_{-27\%}$	5132(24) $^{+5\%}_{-7\%}$	1.03
$Z + 2j$	213(1) $^{+42\%}_{-27\%}$	216(1) $^{+4\%}_{-8\%}$	1.01
$WW(\rightarrow q\bar{q})$	142.2(4) $^{+8\%}_{-7\%}$	221.9(4) $^{+6\%}_{-4\%}$	1.56
$WZ(\rightarrow q\bar{q})$	27.24(8) $^{+9\%}_{-8\%}$	41.8(1) $^{+5\%}_{-5\%}$	1.53
$ZW(\rightarrow q\bar{q})$	5.11(2) $^{+10\%}_{-9\%}$	8.02(7) $^{+6\%}_{-4\%}$	1.57
$t\bar{t}$ (fully- ℓ)	48.5(4) $^{+46\%}_{-28\%}$	59.44(8) $^{+0\%}_{-8\%}$	1.23
$t\bar{t}$ (semi- ℓ)	99.1(7) $^{+47\%}_{-27\%}$	91.7(8) $^{+0\%}_{-11\%}$	0.93
Single t (s)	25.92(4) $^{+10\%}_{-8\%}$	35.6(4) $^{+3\%}_{-3\%}$	1.37
Single t (t)	61.0(1) $^{0\%}_{-2\%}$	49.4(1) $^{-1\%}_{+4\%}$	0.81

Table I: LO and NLO predictions for cross sections using the CDF cuts (exactly two jets). The percentage theoretical uncertainty is estimated by varying the scale choice in the calculation by a factor of two about the central value of $2m_W$. Statistical uncertainty resulting from Monte Carlo integration is shown in parentheses as the error on the final digit.

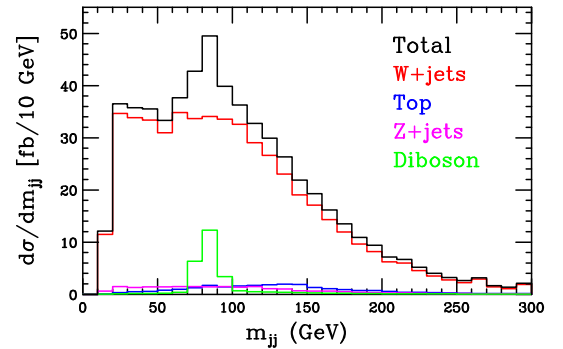


Figure 1: NLO predictions for m_{jj} using the CDF cuts (exactly two jets). The combination of $t\bar{t}$ and single top backgrounds is denoted “Top”, while the contributions from vector boson pairs have been summed and are indicated by “Diboson”.

jet threshold such as $p_T^j > 40$ GeV.

In order to compare our NLO calculations with predictions obtained using tools that are commonly-used experimentally, we present results obtained using a combination of ALPGEN [25] and Pythia [26]. Although only accurate to leading order in the total cross section, the parton shower provides a more realistic environment in which to perform a jet veto. Here we will concentrate on the two most important backgrounds, those from $W +$ jets and top. For the $W +$ jets background we

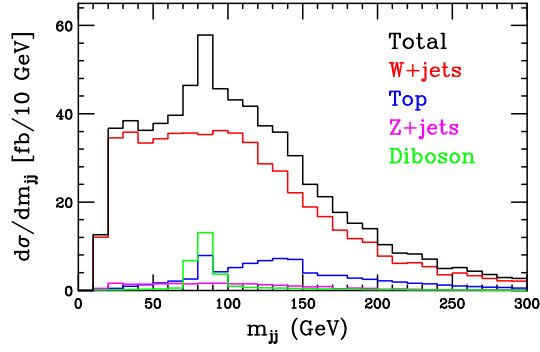


Figure 2: NLO predictions for m_{jj} using the “inclusive” CDF cuts (two or more jets). The labelling is as in Fig. 1.

Process	σ^{LO} [fb]	σ^{NLO} [fb]	Ratio (NLO/LO)
$W + 2j$	4984(8) $^{+41\%}_{-27\%}$	5704(24) $^{+9\%}_{-13\%}$	1.14
$Z + 2j$	213(1) $^{+42\%}_{-27\%}$	236(2) $^{+8\%}_{-12\%}$	1.11
$WW(\rightarrow q\bar{q})$	142.2(4) $^{+8\%}_{-7\%}$	252.3(8) $^{+8\%}_{-6\%}$	1.75
$WZ(\rightarrow q\bar{q})$	27.24(8) $^{+9\%}_{-8\%}$	47.76(12) $^{+8\%}_{-7\%}$	1.75
$ZW(\rightarrow q\bar{q})$	5.11(2) $^{+10\%}_{-9\%}$	9.02(2) $^{+9\%}_{-7\%}$	1.77
$t\bar{t}$ (fully- ℓ)	48.5(4) $^{+46\%}_{-28\%}$	67.1(1) $^{+4\%}_{-11\%}$	1.38
$t\bar{t}$ (semi- ℓ)	686.9(1) $^{+45\%}_{-29\%}$	674.2(1) $^{+3\%}_{-11\%}$	0.98
Single t (s)	25.92(4) $^{+10\%}_{-8\%}$	41.68(4) $^{+7\%}_{-5\%}$	1.61
Single t (t)	61.0(1) $^{0\%}_{-2\%}$	59.8(1) $^{+1\%}_{-0\%}$	0.98

Table II: LO and NLO predictions for cross sections using the “inclusive” CDF cuts (two or more jets). Uncertainties are calculated and indicated in the same fashion as for Table I.

use a matched set of events, while the top backgrounds simply apply the parton shower to a single set of tree-level matrix elements. For the parton shower, particles are formed into jets using the midpoint cone algorithm ($R = 0.4$) via FastJet [27] and we use the CTEQ6L PDF set [28].

We first compare the top distribution under the exclusive and inclusive cuts (with $p_T^j > 30$ GeV) in Fig. 4. To best compare the shapes we have adjusted the distribution obtained from the parton shower such that the W peak is aligned with the parton-level calculation, thus partially correcting for fragmentation and hadronisation effects. As expected from the small corrections to the top processes at NLO, the normalisation of this background is in approximate agreement between the two approaches. However the parton shower gives rise to a somewhat different shape, particularly in the inclusive case where the peak around 140 GeV is broadened.

The other crucial background process is $W + \text{jets}$, for which we compare the results from MCFM and the parton shower in

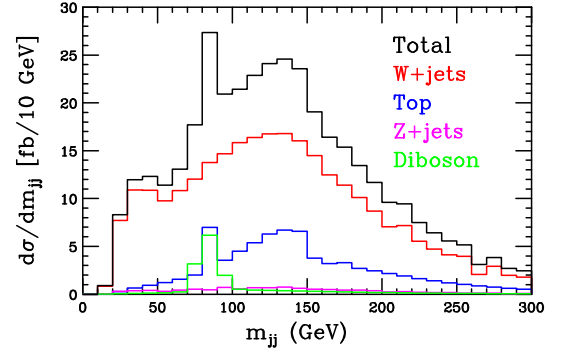


Figure 3: NLO predictions for m_{jj} using the “inclusive” CDF cuts (two or more jets), with an increased jet threshold, $p_T^j > 40$ GeV. The labeling is as in Fig. 1.

Process	σ^{LO} [fb]	σ^{NLO} [fb]	Ratio (NLO/LO)
$W + 2j$	2568(4)	2784(16)	1.08
$Z + 2j$	104.6(8)	112(1)	1.07
$WW(\rightarrow q\bar{q})$	66.6(1)	131.4(4)	1.98
$WZ(\rightarrow q\bar{q})$	14.56(4)	27.96(8)	1.92
$ZW(\rightarrow q\bar{q})$	2.28(1)	4.56(2)	2.00
$t\bar{t}$ (fully- ℓ)	38.2(8)	53.92(8)	1.41
$t\bar{t}$ (semi- ℓ)	655.0(7)	642.2(7)	0.98
Single t (s)	19.44(4)	30.96(4)	1.59
Single t (t)	43.36(8)	42.20(8)	0.97

Table III: LO and NLO cross sections for the $p_T^j > 40$ inclusive final state. Scales are set at $\mu_F = \mu_R = 2m_W$.

Fig. 5. We present the NLO and showered results normalised to their own cross sections so that we can compare the relative shapes. We observe that the change in the shape of the NLO calculation as the scale is varied is small. The prediction from the parton shower has a similar shape as the parton-level results in the tail but differences appear at lower m_{jj} . However this is precisely the region in which we would expect the fixed order calculation to begin to break down and the parton shower to be more reliable.

CONCLUSIONS

We have presented NLO predictions for cross sections and dijet invariant mass distributions for one lepton, missing E_T and two jets at the Tevatron. We have used a variety of cuts, including those used by the CDF collaboration who have recently reported an excess in this distribution around 150 GeV. By calculating the distribution of the invariant mass of the dijets at NLO we have ruled out large NLO K -factors as a

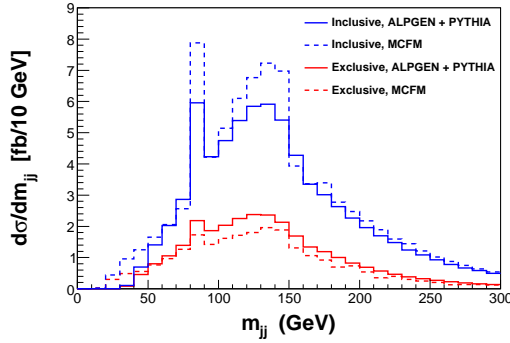


Figure 4: Comparisons of the top backgrounds using MCFM (dashed) and ALPGEN + Pythia (solid) for the exclusive (red) and “inclusive” (blue) cuts.

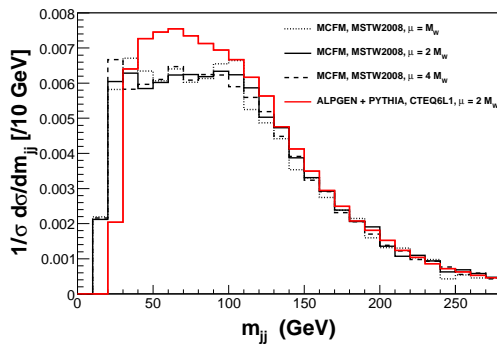


Figure 5: Comparisons of the $W+2j$ backgrounds using MCFM and ALPGEN + Pythia for the “inclusive” cuts. At NLO the dependence of the shape upon the scale choice is shown by the dotted and dashed curves.

possible source of the excess within the context of the SM. At NLO the cross sections have only a moderate dependence on the renormalisation and factorisation scales of QCD, indicating that our results could be used to constrain the overall normalisation of these backgrounds.

The SM predicts a parton-level edge in the top background around 150 GeV, an edge that is softened into a broader peak by the parton shower. Detector effects, that we have not considered here, will certainly modify this feature further. In order to gain better control over the shape of this background we would advocate the use of the more inclusive cuts for which the top background is much larger and thus more easily constrained. It becomes even more significant for cuts demanding harder jets. For instance a $p_T^j > 40$ GeV cut yields a top cross section in the region of the broad peak only a factor of 2.5 lower than the W + jets contribution. Further information on this background could be gleaned by investigating the dijet mass distribution for the case of b -tagged (or anti-tagged) jets. In particular, the dominant source of two anti- b -tagged jets is

from the hadronic decay of the W . The invariant mass of two anti- b -tagged jets should therefore peak sharply around m_W , with no significant peak in the 100–150 GeV region.

ACKNOWLEDGMENTS

We thank Viviana Cavaliere, Keith Ellis, Walter Giele, Roni Harnik, Joey Huston, Graham Kribs, Fabio Maltoni and Zack Sullivan and Jan Winter for useful discussions. Fermilab is operated by Fermi Research Alliance, LLC under Contract No. DE-AC02-07CH11359 with the United States Department of Energy.

-
- [1] T. Aaltonen et al. (CDF) (2011), 1104.0699.
 - [2] E. J. Eichten, K. Lane, and A. Martin (2011), 1104.0976.
 - [3] M. R. Buckley, D. Hooper, J. Kopp, and E. Neil (2011), 1103.6035.
 - [4] F. Yu (2011), 1104.0243.
 - [5] C. Kilic and S. Thomas (2011), 1104.1002.
 - [6] K. Cheung and J. Song (2011), 1104.1375.
 - [7] X.-G. He and B.-Q. Ma (2011), 1104.1894.
 - [8] X.-P. Wang, Y.-K. Wang, B. Xiao, J. Xu, and S.-h. Zhu (2011), 1104.1917.
 - [9] R. Sato, S. Shirai, and K. Yonekura (2011), 1104.2014.
 - [10] A. E. Nelson, T. Okui, and T. S. Roy (2011), 1104.2030.
 - [11] L. A. Anchordoqui, H. Goldberg, X. Huang, D. Lust, and T. R. Taylor (2011), 1104.2302.
 - [12] B. A. Dobrescu and G. Z. Krnjaic (2011), 1104.2893.
 - [13] P. Ko, Y. Omura, and C. Yu (2011), 1104.4066.
 - [14] P. J. Fox, J. Liu, D. Tucker-Smith, and N. Weiner (2011), 1104.4127.
 - [15] D.-W. Jung, P. Ko, and J. S. Lee (2011), 1104.4443.
 - [16] S. Chang, K. Y. Lee, and J. Song (2011), 1104.4560.
 - [17] B. Bhattacharjee and S. Raychaudhuri (2011), 1104.4749.
 - [18] Q.-H. Cao et al. (2011), 1104.4776.
 - [19] L. M. Carpenter and S. Mantry (2011), 1104.5528.
 - [20] T. Enkhbat, X.-G. He, Y. Mimura, and H. Yokoya (2011), 1105.2699.
 - [21] T. Plehn and M. Takeuchi (2011), 1104.4087.
 - [22] Z. Sullivan and A. Menon (2011), 1104.3790.
 - [23] J. M. Campbell, R. K. Ellis, and C. Williams (2011), 1105.0020.
 - [24] A. D. Martin, W. J. Stirling, R. S. Thorne, and G. Watt, Eur. Phys. J. **C63**, 189 (2009), 0901.0002.
 - [25] M. L. Mangano, M. Moretti, F. Piccinini, R. Pittau, and A. D. Polosa, JHEP **07**, 001 (2003).
 - [26] T. Sjostrand, S. Mrenna, and P. Skands, JHEP **05**, 026 (2006), hep-ph/0603175.
 - [27] M. Cacciari and G. P. Salam, Phys. Lett. **B641**, 57 (2006), hep-ph/0512210.
 - [28] J. Pumplin, D. Stump, J. Huston, H. Lai, P. M. Nadolsky, et al., JHEP **0207**, 012 (2002), hep-ph/0201195.
 - [29] In this letter we neglect $ZZ(\rightarrow q\bar{q})$ since its contribution in the mass range of interest is negligible.